Baby Skyrmions on the two-sphere

Itay Hen* and Marek Karliner†
Raymond and Beverly Sackler School of Physics and Astronomy, Tel-Aviv University, Tel-Aviv 69978, Israel
(Received 4 December 2007; revised manuscript received 15 January 2008; published 25 March 2008)

We find the static multisoliton solutions of the baby Skyrme model on the two-sphere for topological charges $1 \leq B \leq 14$. Numerical full-field results show that the charge-one Skyrmion is spherical, the charge-two Skyrmion is toroidal, and Skyrmions with higher charge all have point symmetries which are subgroups of O(3). We find that a rational map ansatz yields very good approximations to the full-field solutions. We point out a strong connection between the discrete symmetries of our solutions and those of corresponding solutions of the three-dimensional Skyrme model.

DOI: 10.1103/PhysRevE.77.036612 PACS number(s): 03.50.−z, 12.39.Dc, 11.27.+d

I. INTRODUCTION

The Skyrme model [1] is a nonlinear theory of pions in (3+1) dimensions with topological soliton solutions called Skyrmions. The existence of stable solutions in this model is a consequence of the nontrivial topology of the mapping $\mathcal{M}$ of the physical space into the field space at a given time, $\mathcal{M}: S^3 \to \mathrm{SU}(2) \cong S^3$, where the physical space $\mathbb{R}^3$ is compactified to S^3 by requiring the spatial infinity to be equivalent in each direction. The topology which stems from this one-point compactification allows the classification of maps into equivalence classes, each of which has a unique conserved quantity called the topological charge.

Although Skyrmions were originally introduced to describe baryons in three spatial dimensions [1], they have been shown to exist for a very wide class of geometries [2], and are now playing an increasing role in other areas of physics as well.

Apart from the original three-dimensional (3D) model, which exhibits very structured solitonic solutions (for a review see [3]), other Skyrme models are known to yield solutions with intricate structures. The baby Skyrme model, first introduced by [4], is a two-dimensional version of the original Skyrme model, with $\mathbb{R}^2$ as its domain. As its older brother, it is known to give rise, under certain settings, to structured multi-Skyrmion configurations [4–8]. Studies of other Skyrme models defined on curved domains, such as cylinders, two-spheres, and three-spheres can also be found in the literature [9–13]. Although most of these models are used as a simplification or as "toy" models of the full 3D model, they also have physical significance on their own, having several applications in condensed-matter physics, specifically in context of quantum Hall systems [14,15], where they arise as low-energy excitations near ferromagnetic filling factors.

In the present paper we consider a baby Skyrme model on the two-sphere. This type of model has been studied in [10,11], where only rotationally symmetric configurations have been considered. We compute the full-field minimal energy solutions of the model up to charge 14 and show that they exhibit complex multi-Skyrmion solutions closely related to the Skyrmion solutions of the 3D model with the same topological charge. To obtain the minimum energy configurations, we apply two completely different methods. One is a full-field relaxation method, with which exact numerical solutions of the model are obtained. The other approach is a rational map approximation scheme, which as we show yields very good approximate solutions. We discuss these methods in detail in Sec. III.

In an exact analogy to the 3D Skyrme model, our results show that the charge-one Skyrmion has a spherical energy distribution, the charge-two Skyrmion is toroidal, and Skyrmions with higher charge all have point symmetries which are subgroups of O(3). The symmetries of these solutions are the same as those of the 3D Skyrmions. As we shall see, this is not a coincidence.

II. BABY SKYRME MODEL ON THE TWO-SPHERE

The model in question is a baby Skyrme model in which both the domain and target are two-spheres. It consists of a triplet of real scalar fields $\boldsymbol{\phi}=(\phi_1,\phi_2,\phi_3)$ subject to the constraint $\boldsymbol{\phi}\boldsymbol{\phi}=1$. The Lagrangian density is simply

$$\mathcal{L} = \frac{1}{2}\partial_\mu \boldsymbol{\phi}\partial^\mu \boldsymbol{\phi} + \frac{\kappa^2}{2}[(\partial_\mu \boldsymbol{\phi}\partial^\mu \boldsymbol{\phi})^2 - (\partial_\mu \boldsymbol{\phi}\partial_\nu \boldsymbol{\phi})(\partial^\mu \boldsymbol{\phi}\partial^\nu \boldsymbol{\phi})], \tag{1}$$

with metric $ds^2=dt^2-d\theta^2-\sin^2\theta d\varphi^2$, where θ is the polar angle $\in[0,\pi]$ and φ is the azimuthal angle $\in[0,2\pi)$. The Lagrangian of this model is invariant under rotations in both the domain and the target spaces, possessing an $O(3)_{\mathrm{domain}} \times O(3)_{\mathrm{target}}$ symmetry. The first term in the Lagrangian is the kinetic term and the second term, of the fourth order in derivatives, is the 2D analog of the Skyrme term [4]. In flat two-dimensional space a third potential term is necessary to ensure the existence of stable finite-size solutions. Without it, the repulsive effect of the Skyrme term causes the Skyrmions to expand indefinitely. In the present model, however, the finite geometry of the sphere acts as a stabilizer, so a potential term is not required. Furthermore, stable solutions exist even without the Skyrme term. In the latter case, we obtain the well known $O(3)$ (or $\mathbb{CP}^1$) nonlinear sigma model [16].

The field $\boldsymbol{\phi}$ in this model is an $S^2 \to S^2$ mapping. The relevant homotopy group of this model is $\pi_2(S^2)=\mathbb{Z}$, which

*itayhe@post.tau.ac.il
†marek@proton.tau.ac.il

implies that each field configuration is characterized by an integer topological charge B, the topological degree of the map $\boldsymbol{\phi}$, which in spherical coordinates is given by

$$B = \frac{1}{4\pi}\int d\Omega \frac{\boldsymbol{\phi}(\partial_\theta \boldsymbol{\phi} \times \partial_\varphi \boldsymbol{\phi})}{\sin\theta}, \tag{2}$$

where $d\Omega = \sin\theta d\theta d\varphi$.

Static solutions within each topological sector are obtained by minimizing the energy functional

$$E = \frac{1}{2}\int d\Omega \left((\partial_\theta \boldsymbol{\phi})^2 + \frac{1}{\sin^2\theta}(\partial_\varphi \boldsymbol{\phi})^2 \right) + \frac{\kappa^2}{2}\int d\Omega \left(\frac{(\partial_\theta \boldsymbol{\phi} \times \partial_\varphi \boldsymbol{\phi})^2}{\sin^2\theta} \right). \tag{3}$$

Before proceeding, it is worth noting here that setting $\kappa = 0$ in Eq. (3) yields the energy functional of the $O(3)$ nonlinear sigma model. The latter has analytic minimal energy solutions within every topological sector, given by

$$\boldsymbol{\phi} = [\sin f(\theta)\cos(B\varphi), \sin f(\theta)\sin(B\varphi), \cos f(\theta)], \tag{4}$$

where $f(\theta) = \cos^{-1}\{1 - 2[1 + (\lambda \tan\theta/2)^{2B}]^{-1}\}$ with λ being some positive number [16]. These solutions are not unique, as other solutions with the same energy may be obtained by rotating Eq. (4) either in the target or in the domain spaces. The energy distributions of these solutions in each sector are rotationally symmetric, with total energy $E_B = 4\pi B$.

We have found that analytic solutions also exist for the energy functional (3) with the Skyrme term only. They too have the rotationally symmetric form (4) with $f(\theta) = \theta$ and total energy $E_B = 4\pi B^2$. They can be shown to be the global minima by the following Cauchy-Schwartz inequality:

$$\left(\frac{1}{4\pi}\int d\Omega \frac{\boldsymbol{\phi}(\partial_\theta \boldsymbol{\phi} \times \partial_\varphi \boldsymbol{\phi})}{\sin\theta} \right)^2 \leq \left(\frac{1}{4\pi}\int d\Omega \boldsymbol{\phi}^2 \right) \left[\frac{1}{4\pi}\int d\Omega \left(\frac{\partial_\theta \boldsymbol{\phi} \times \partial_\varphi \boldsymbol{\phi}}{\sin\theta} \right)^2 \right]. \tag{5}$$

The left-hand side is simply B^2 and the first term in parentheses on the right-hand side integrates to 1. Noting that the second term in the right-hand side is the Skyrme energy (without the $\kappa^2/2$ factor), the inequality reads $E \geq 4\pi B^2$, with equality for the rotationally symmetric solutions.

III. STATIC SOLUTIONS

In general, if both the kinetic and Skyrme terms are present, static solutions of the model cannot be obtained analytically. The Euler-Lagrange equations derived from the energy functional (3) are nonlinear PDE's, so the minimal energy configurations can only be obtained with the aid of numerical techniques. This is with the exception of the $B = 1$ Skyrmion, which has an analytic "hedgehog" solution

$$\boldsymbol{\phi}_{[B=1]} = (\sin\theta\cos\varphi, \sin\theta\sin\varphi, \cos\theta), \tag{6}$$

with total energy $\frac{E}{4\pi} = 1 + \frac{\kappa^2}{2}$.

For Skyrmions with higher charge, we find the minimal energy configurations by utilizing a full-field relaxation method, described in more detail below. In parallel, we also apply the rational map approximation method, originally developed for the 3D Skyrme model and directly compare the results with the relaxation method. This method is also discussed below.

A. Full-field relaxation method

For the relaxation method, the domain S^2 is discretized to a spherical grid—100 grid points for θ and 100 points for φ. The relaxation process begins by initializing the field triplet $\boldsymbol{\phi}$ to a rotationally symmetric configuration

$$\boldsymbol{\phi}_{\text{initial}} = (\sin\theta\cos B\varphi, \sin\theta\sin B\varphi, \cos\theta), \tag{7}$$

where B is the topological charge of the Skyrmion in question. The energy of the baby Skyrmion is then minimized by repeating the following steps: a point (θ_m, φ_n) on the grid is chosen at random, along with one of the three components of the field $\boldsymbol{\phi}(\theta_m, \varphi_n)$. The chosen component is then shifted by a value $\delta_{\boldsymbol{\phi}}$ chosen uniformly from the segment $[-\Delta_{\boldsymbol{\phi}}, \Delta_{\boldsymbol{\phi}}]$ where $\Delta_{\boldsymbol{\phi}} = 0.1$ initially. The field triplet is then normalized and the change in energy is calculated. If the energy decreases, the modification of the field is accepted and otherwise it is discarded. The procedure is repeated while the value of $\Delta_{\boldsymbol{\phi}}$ is gradually decreased throughout the procedure. This is done until no further decrease in energy is observed.

One undesired feature of this minimization scheme is that it can get stuck at a local minimum. This problem can be resolved by using the "simulated annealing" algorithm [17,18], which in fact has been successfully implemented before, in obtaining the minimal energy configurations of static two- and three-dimensional Skyrmions [19]. The algorithm is comprised of repeated applications of a Metropolis algorithm with a gradually decreasing temperature, based on the fact that when a physical system is slowly cooled down, reaching thermal equilibrium at each temperature, it will end up in its ground state. This algorithm, however, is much more expensive in terms of computer time. We therefore employ it only in part, just as a check on our results, which correspond to a Metropolis algorithm of zero temperature.

As a further verification, we set up the minimization scheme using different initial configurations and grids of different sizes (80×80 and 200×200) for several κ and B values. This was done to make sure that the final configurations are independent of the discretization and cooling scheme. Accuracy was also verified by checking the conservation of the topological charge B throughout the minimization process, yielding $\left|\frac{B_{\text{observed}}}{B} - 1\right| < 10^{-6}$.

B. Rational map ansatz

Computing the minimum energy configurations using the full nonlinear energy functional is a procedure which is both time consuming and resource hungry. To circumvent these problems, the rational map ansatz scheme has been devised. First introduced in [20], this scheme has been used in obtaining approximate solutions to the 3D Skyrme model using rational maps between Riemann spheres. Although this representation is not exact, it drastically reduces the number of

degrees of freedom in the problem, allowing computations to take place in a relatively short amount of time. The results in the case of the 3D Skyrme model are known to be quite accurate.

Application of the approximation begins with expressing points on the base sphere by the Riemann sphere coordinate $z=\tan\frac{\theta}{2}e^{i\varphi}$. The complex-valued function $R(z)$ is a rational map of degree B between Riemann spheres

$$R(z)=\frac{p(z)}{q(z)}, \tag{8}$$

where $p(z)$ and $q(z)$ are polynomials in z, such that $\max[\deg(p),\deg(q)]=B$, and p and q have no common factors. Given such a rational map, the ansatz for the field triplet is

$$\boldsymbol{\phi}=\left(\frac{R+\bar{R}}{1+|R|^2},i\frac{R-\bar{R}}{1+|R|^2},\frac{1-|R|^2}{1+|R|^2}\right). \tag{9}$$

It can be shown that rational maps of degree B correspond to field configurations with charge B [20]. Substitution of the ansatz (9) into the energy functional (3) results in the simple expression

$$\frac{1}{4\pi}E=B+\frac{\kappa^2}{2}\mathcal{I}, \tag{10}$$

with

$$\mathcal{I}=\frac{1}{4\pi}\int\left(\frac{1+|z|^2}{1+|R|^2}\left|\frac{dR}{dz}\right|\right)^4\frac{2idzd\bar{z}}{(1+|z|^2)^2}. \tag{11}$$

Note that in the $\kappa\to 0$ limit, where our model reduces to the $O(3)$ nonlinear sigma model, the rational maps become, in fact, exact solutions and the minimal energy value $E=4\pi B$ is attained. Furthermore, the minimal energy is reached independently of the specific details of the map (apart from its degree), i.e., all rational maps of a given degree are minimal energy configurations in the topological sector corresponding to this degree. This is a reflection of the scale and the rotational invariance of the $O(3)$ model.

In the general case where $\kappa\neq 0$, the situation is different. Here, minimizing the energy (10) requires finding the rational map which minimizes the functional $\mathcal{I}$. As we discuss in the next section, the expression for $\mathcal{I}$ given in Eq. (11) is encountered in the application of the rational map in the context of 3D Skyrmions, where the procedure of minimizing $\mathcal{I}$ over all rational maps of the various degrees has been used [20–22].

Here we redo the calculations, using a relaxation method. To obtain the rational map of degree B that minimizes $\mathcal{I}$, we start off with a rational map of degree B, with the real and imaginary parts of the coefficients of $p(z)$ and $q(z)$ assigned random values from the segment $[-1,1]$. As in the full-field relaxation method discussed above, solutions are obtained by relaxing the map until a minimum of $\mathcal{I}$ is reached.

IV. RELATION TO THE 3D SKYRME MODEL

In the 3D Skyrme model, the rational map ansatz can be thought of as taken in two steps. First, the radial coordinate is separated from the angular coordinates by taking the SU(2) Skyrme field $U(r,\theta,\varphi)$ to be of the form

$$U(r,\theta,\varphi)=\exp[if(r)\boldsymbol{\phi}(\theta,\varphi)\cdot\boldsymbol{\sigma}], \tag{12}$$

where $\boldsymbol{\sigma}=(\sigma_1,\sigma_2,\sigma_3)$ are Pauli matrices, $f(r)$ is the radial profile function subject to the boundary conditions $f(0)=\pi$ and $f(\infty)=0$, and $\boldsymbol{\phi}(\theta,\varphi)$: $S^2\mapsto S^2$ is a normalized vector which carries the angular dependence of the field. In terms of the ansatz (12), the energy of the Skyrme field is

$$E=\int 4\pi f'^2r^2dr+\int 2(f'^2+1)\sin^2 f dr\int\left((\partial_\theta\boldsymbol{\phi})^2+\frac{1}{\sin^2\theta}(\partial_\varphi\boldsymbol{\phi})^2\right)d\Omega+\int\frac{\sin^4 f}{r^2}dr\int\frac{(\partial_\theta\boldsymbol{\phi}\times\partial_\varphi\boldsymbol{\phi})^2}{\sin^2\theta}d\Omega. \tag{13}$$

Note that the energy functional (13) is actually the energy functional of our model (3) once the radial coordinate is integrated out. Thus, our 2D model can be thought of as a 3D Skyrme model with a frozen radial coordinate.

The essence of the rational map approximation is the assumption that $\boldsymbol{\phi}(\theta,\varphi)$ takes the rational map form (9), which in turn leads to a simple expression for the energy

$$E=4\pi\int\left(r^2f'^2+2B(f'^2+1)\sin^2 f+\mathcal{I}\frac{\sin^4 f}{r^2}\right)dr, \tag{14}$$

where $\mathcal{I}$ is given in Eq. (11). As in our case, minimizing the energy functional requires [as a first step, followed by finding the profile function $f(r)$] minimizing $\mathcal{I}$ over all maps of degree B.

Since the symmetries of the 3D Skyrmions are determined solely by the angular dependence of the Skyrme field, it should not be too surprising that the solutions of the model discussed here share the symmetries of the corresponding solutions of the 3D Skyrme model.

V. RESULTS

The two approaches discussed in Sec. III have been applied separately to obtain the static solutions for charges $2\leq B\leq 14$ (the charge-one solution has an analytic representation, as discussed in Sec. III). This was done for several κ values within the range $0.01\leq\kappa^2\leq 0.2$, although solutions with different κ's turned out to be qualitatively similar, as will be discussed at the end of this section.

As discussed in the previous section, the configurations obtained from the full-field relaxation method were found to have the same symmetries as corresponding multi-Skyrmions of the 3D model with the same charge. The $B=2$ solution turned out to be axially symmetric, whereas higher-charge solutions were all found to have point symmetries which are subgroups of O(3). For $B=3$ and $B=12$, the Skyrmions have a tetrahedral symmetry. The $B=4$ and $B=13$ Skyrmions have a cubic symmetry, and the $B=7$ is dodecahedral. The other Skyrmion solutions have dihedral symmetries: For $B=5$ and $B=14$ a D_{2d} symmetry, for $B=6$, 9, and 10 a D_{4d} symmetry, for $B=8$ a D_{6d} symmetry, and for $B=11$ a D_{3h} symmetry. In Fig. 1 we show the energy distri-

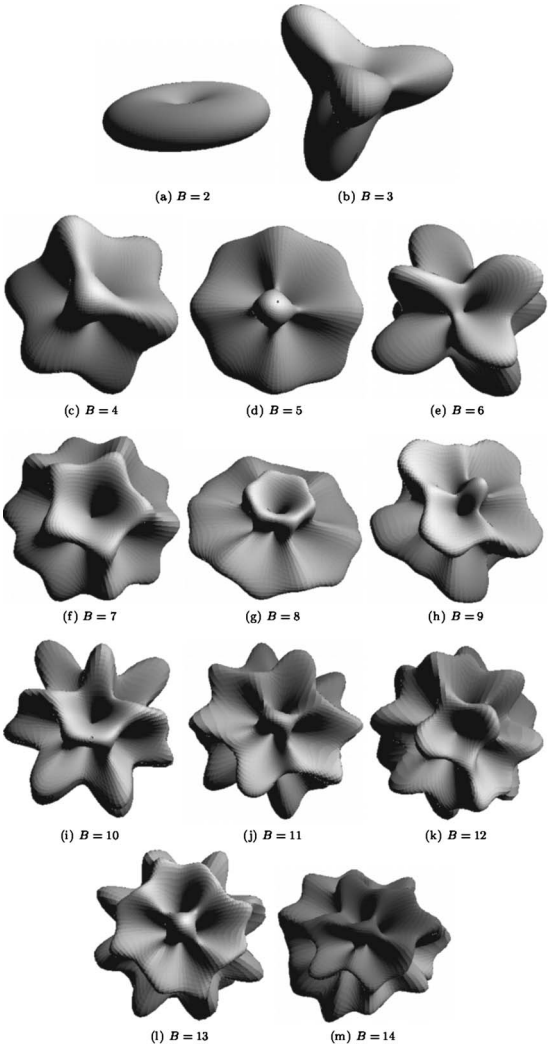

FIG. 1. The energy distributions of the multi-Skyrmion solutions for charges $2 \leq B \leq 14$ ($\kappa^2 = 0.05$).

butions of the obtained solutions for $\kappa^2 = 0.05$, and in Fig. 2 we plot the actual fields of the lower-charge solutions.

While for solutions with $B < 8$ the energy density (and also the charge density) is distributed in distinct peaks, for solutions with higher charge it is spread in a much more complicated manner. The total energies of the solutions (divided by $4\pi B$) are listed in Table I, along with the symmetries of the solutions (again with $\kappa^2 = 0.05$).

Application of the rational map ansatz yielded results with only slightly higher energies, only about 0.3%–3% above the full-field results. The calculated values of $\mathcal{I}$ were found to agree with those obtained in [21] in the context of 3D Skyrmions. For $9 \leq B \leq 14$, the rational map approximation yielded slightly less symmetric solutions than the full-field ones. Considering the relatively small number of degrees of freedom, this method all-in-all yields very good approximations. The total energies of the solutions obtained with the rational map approximation is also listed in Table I.

The effect of the parameter κ on the solutions of the model is best understood if one first considers the effect of rescaling on the energy functional (3). Assigning an arbitrary radius r to the base sphere, the kinetic term is found to be

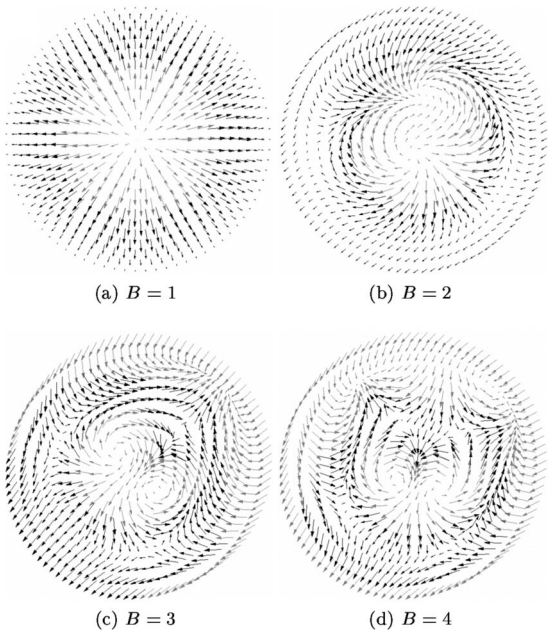

FIG. 2. Plots of the field configurations $\boldsymbol{\phi}$ in charge sectors $1 \leq B \leq 4$. Here, the base sphere is mapped to a circle and the arrows represent the first two components of the field triplet, namely, (ϕ_1, ϕ_2). The color of the arrows represents the sign of ϕ_3; black for negative values and gray otherwise.

invariant, whereas the Skyrme term, proportional to κ^2, scales like $\sim r^{-2}$. Hence κ has the role of the inverse of the radius of the sphere; large values of κ correspond to a small sphere, and vice versa. In accord with the above arguments, numerical results indicate that increasing the value of κ (or alternatively shrinking the base sphere), results in the energy-density peaks becoming smeared. The Skyrmions, having less space for themselves, superimpose, and as a consequence, distort one another. The symmetries of the obtained solutions, however, remain the same. The above is

TABLE I. Total energies (divided by $4\pi B$) of the multisolitons of the model for $\kappa^2 = 0.05$.

Charge B	Total energy (full-field)	Total energy (rational maps)	Difference in %	Symmetry of the solution
2	1.071	1.073	0.177	Toroidal
3	1.105	1.113	0.750	Tetrahedral
4	1.125	1.129	0.359	Cubic
5	1.168	1.179	0.958	D_{2d}
6	1.194	1.211	1.426	D_{4d}
7	1.209	1.217	0.649	Icosahedral
8	1.250	1.268	1.406	D_{6d}
9	1.281	1.304	1.771	D_{4d}
10	1.306	1.332	1.991	D_{4d}
11	1.337	1.366	2.224	D_{3h}
12	1.360	1.388	2.072	Tetrahedral
13	1.386	1.415	2.137	Cubic
14	1.421	1.459	2.712	D_2

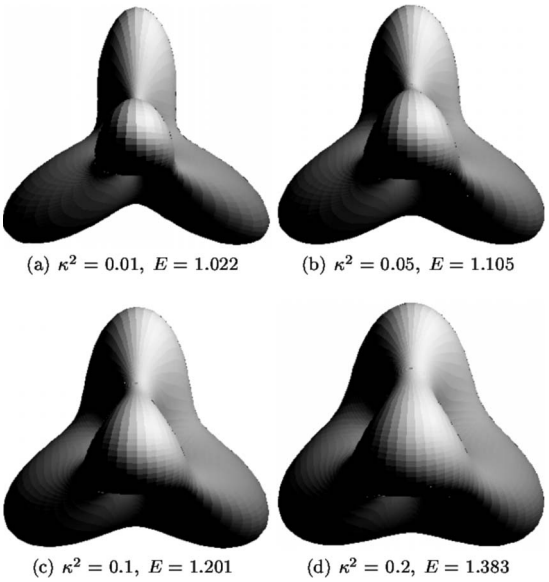

FIG. 3. The energy distributions of the $B=3$ Skyrmion solution for different values of κ. As κ increases, the peaks become smeared but the symmetry of the solution is unaffected. The total energies of the solutions (divided by 12π) are also shown.

illustrated in Fig. 3, where we have plotted the energy distribution of the $B=3$ Skyrmion for different values of κ.

VI. SUMMARY AND CONCLUSION

We have studied the baby Skyrme model on the two-sphere, obtaining the minimal energy configurations for all charges up to $B=14$, using both the full-field relaxation method and the rational map approximation scheme. For each charge we have identified the symmetry and measured the energy of the minimal energy Skyrmion. The solutions turned out to yield very structured configurations, exhibiting the same symmetries as the corresponding solutions of the 3D Skyrme model.

We have explained the reason for these similarities between the symmetries of the two models and in the process we have exhibited a strong connection between them. The model discussed in this paper may be thought of as the 3D Skyrme model with a frozen radial coordinate. In that sense, our computations may serve as an additional corroboration of results obtained for the 3D Skyrmions.

In addition, we have shown that the rational map ansatz provides a very good approximate description to the true solutions, also for those with high topological charge. The energies of the solutions computed in the rational maps approximation are only slightly higher than the full-field solutions, and their symmetries, in most cases, are the same. This suggests that rational maps may be used to construct good approximations to multi-Skyrmion solutions in this model in a rather simple way.

We believe that this work may provide a useful tool in the study of 3D Skyrmions, as our model shares great similarities with the 3D model, especially in terms of multi-Skyrmion symmetries. The fact that the model discussed here is two dimensional makes it simpler to study and perform computations with, when compared with the 3D Skyrme model.

Some of the results obtained in the present work may, at least to some extent, also be linked to the baby Skyrmions which appear in two-dimensional electron gas systems, exhibiting the quantum Hall effect. As briefly noted in the Introduction, baby Skyrmions arise in quantum Hall systems as low-energy excitations of the ground state, near ferromagnetic filling factors (notably 1 and 1/3) [14,15]. There, the Skyrmion is a twisted two-dimensional configuration of spin, and its topological charge corresponds to the number of times the spin rotates by 2π. While for the electron gas, the stability of the soliton arises from a balance between the electron-electron Coulomb energy and the Zeeman energy, in our model the repulsive Skyrme-term energy is balanced by the underlying geometry (i.e., the sphere). The connection between these two models suggests the possible existence of very structured spin textures in quantum Hall systems, although a more detailed analysis of this analogy is in order. We hope to be able to report on these matters in forthcoming publications.

ACKNOWLEDGMENTS

We thank Wojtek Zakrzewski for useful discussions. This work was supported in part by a grant from the Israel Science Foundation administered by the Israel Academy of Sciences and Humanities.

[1] T. H. R. Skyrme, Proc. R. Soc. London, Ser. A **260**, 127 (1961); Nucl. Phys. **31**, 556 (1962).
[2] N. S. Manton, Commun. Math. Phys. **111**, 469 (1987).
[3] N. S. Manton and P. M. Sutcliffe, *Topological Solitons* (Cambridge University Press, Cambridge, 2004), Chap. 9.
[4] B. M. A. G. Piette, B. J. Schoers, and W. J. Zakrzewski, Z. Phys. C **65**, 165 (1995).
[5] B. M. A. G. Piette, B. J. Schoers, and W. J. Zakrzewski, Nucl. Phys. B **439**, 205 (1995).
[6] R. A. Leese, M. Peyrard, and W. J. Zakrzewski, Nonlinearity **3**, 773 (1990).
[7] B. M. A. G. Piette and W. J. Zakrzewski, Chaos, Solitons Fractals **5**, 2495 (1995).
[8] P. M. Sutcliffe, Nonlinearity **4**, 1109 (1991).
[9] R. Dandoloff and A. Saxena, Eur. Phys. J. B **29**, 265 (2002).
[10] M. de Innocentis and R. S. Ward, Nonlinearity **14**, 663 (2001).
[11] N. N. Scoccola and D. R. Bes, J. High Energy Phys. 09, (1998) 012.
[12] A. Wirzba and H. Bang, Nucl. Phys. A **515**, 571 (1990).
[13] S. Krusch, Nonlinearity **13**, 2163 (2000).
[14] S. L. Sondhi, A. Karlhede, S. A. Kivelson, and E. H. Rezayi, Phys. Rev. B **47**, 16419 (1993).

[15] J. G. Groshaus, I. Dujovne, Y. Gallais, C. F. Hirjibehedin, A. Pinczuk, Y. W. Tan, H. Stormer, B. S. Dennis, L. N. Pfeiffer, and K. W. West, Phys. Rev. Lett. **100**, 046804 (2008).
[16] A. A. Belavin and A. M. Polyakov, JETP Lett. **22**, 245 (1975).
[17] S. Kirkpatrick, C. D. Gellat, and M. P. Vecchi, Science **220**, 671 (1983).
[18] S. Geman and D. Geman, IEEE Trans. Pattern Anal. Mach. Intell. **6**, 721 (1984).
[19] M. Hale, O. Schwindt, and T. Weidig, Phys. Rev. E **62**, 4333 (2000).
[20] C. J. Houghton, N. S. Manton, and P. M. Sutcliffe, Nucl. Phys. B **510**, 507 (1998).
[21] R. A. Battye and P. M. Sutcliffe, Rev. Math. Phys. **14**, 29 (2002).
[22] N. S. Manton and B. M. A. G. Piette, e-print arXiv:hep-th/0008110.